

---

---

# Serial $^{18}\text{F}$ -FDG PET Demonstrates Benefit of Human Mesenchymal Stem Cells in Treatment of Intracerebral Hematoma: A Translational Study in a Primate Model

Ming Feng<sup>1\*</sup>, Hua Zhu<sup>2\*</sup>, Zhaohui Zhu<sup>3\*</sup>, Junji Wei<sup>1\*</sup>, Shan Lu<sup>4</sup>, Qin Li<sup>3</sup>, Nan Zhang<sup>5</sup>, Guilin Li<sup>1</sup>, Fang Li<sup>3</sup>, Wenbin Ma<sup>1</sup>, Yihua An<sup>6</sup>, Robert Chunhua Zhao<sup>4</sup>, Chuan Qin<sup>3</sup>, and Renzhi Wang<sup>1</sup>

<sup>1</sup>Department of Neurosurgery of Peking Union Medical College Hospital, Chinese Academy of Medical Science and Peking Union Medical College, Beijing, China; <sup>2</sup>Institute of Laboratory Animal Sciences, Chinese Academy of Medical Science and Peking Union Medical College, Beijing, China; <sup>3</sup>Department of Nuclear Medicine of Peking Union Medical College Hospital, Chinese Academy of Medical Science and Peking Union Medical College, Beijing, China; <sup>4</sup>Institute of Basic Medical Sciences, Chinese Academy of Medical Science and Peking Union Medical College; <sup>5</sup>Coal General Hospital, Beijing, China; and <sup>6</sup>Beijing Neurosurgical Institute, Beijing, China

---

This study evaluated the efficacy of human mesenchymal stem cells (hMSCs) in the treatment of intracerebral hematoma (ICH) using a primate model and serial  $^{18}\text{F}$ -FDG PET scans. **Methods:** Twenty-four *Macaca fascicularis* monkeys (male,  $4.2 \pm 0.2$  kg) were enrolled. The ICH models were established using a stereo-guided injection of 1.5 mL of autologous arterial blood between the right cortex and basal ganglia. One week (early treatment group,  $n = 8$ ) or 4 wk (late treatment group,  $n = 8$ ) after an ICH was established,  $(1-5) \times 10^6$  hMSCs were transplanted near the hematoma using a stereotactic method. Control monkeys received saline only, either 1 or 4 wk ( $n = 4$  for each subgroup) after ICH establishment. The efficacy of treatment was evaluated by serial  $^{18}\text{F}$ -FDG PET scans ( $n = 19$ ) and neurologic deficit scoring weekly or biweekly. Pathologic analysis was performed 8 wk after hMSC transplantation. **Results:** One week after hMSC injection, higher  $^{18}\text{F}$ -FDG accumulated at the ipsilateral basal ganglia in both early and late hMSC-treated groups, indicating an early response to the treatment. When recovery reached a plateau,  $^{18}\text{F}$ -FDG uptake in the adjacent cortex was significantly higher in the early treatment group ( $P < 0.05$ ). The neurologic deficit scoring was significantly lower in the hMSC-treated groups, which also indicated better recovery. Pathologic analysis revealed higher vessel density surrounding the remains of hematoma in the hMSC-treated groups. **Conclusion:** This preliminary study indicates that transplantation of hMSCs may improve the recovery from ICH in a primate model, and early treatment may lead to better results.

**Key Words:** intracerebral hematoma; mesenchymal stem cells; transplantation; *Macaca fascicularis*; positron emission tomography

J Nucl Med 2011; 52:90–97

DOI: 10.2967/jnumed.110.080325

**I**ntracerebral hematoma (ICH) after cerebrovascular disease is a serious threat to human health. Intracerebral hemorrhage accounts for 10%–15% of all cases of stroke (1), with a 30-d mortality ranging from 35% to 52% (2,3). Nearly 30% of patients with ischemic stroke have secondary cerebral hemorrhage (4), and a significant number of patients will develop cerebral hemorrhage after thrombolytic therapy (5). The management of patients with an ICH is generally limited to supportive care or evacuation of the hematoma; the efficacy of surgical removal of hematoma is variable and controversial (1–3).

Stem cell transplantation holds the promise of a cure for many degenerative diseases, including cerebrovascular disease. Human mesenchymal stem cells (hMSCs), usually obtained from bone marrow, are multipotent stem cells. hMSCs have many advantages over other stem cells, such as embryonic stem cells. Human mesenchymal cells have low immunogenicity, arouse fewer ethical disputes, allow for autografting, and show positive immunomodulation effects. Stem cell treatment has shown benefits in a few studies using experimental ICH models in rodents (6–12), but no comparative study has been reported in primates. In this study, an experimentally induced ICH model was established in the *Macaca fascicularis* monkey. Serial PET scans, with  $^{18}\text{F}$ -FDG as the tracer, were used to evaluate the metabolic recovery of surrounding cortex and basal ganglia of the monkey brains and were correlated with the recovery of neurologic function deficit and with pathologic findings.

## MATERIALS AND METHODS

### Cell Preparation

Bone marrow (20 mL per person) was collected from healthy adult human volunteers. The volunteers signed a declaration of informed consent before surgery. The hMSCs were isolated and cultured as described in a previous report (13), and the method is briefly described below.

---

Received Jun. 25, 2010; revision accepted Oct. 18, 2010.

For correspondence or reprints contact: Renzhi Wang, Department of Neurosurgery of Peking Union Medical College Hospital, 100730, Beijing, P.R. China.

E-mail: wangrz@126.com

\*Contributed equally to this work.

COPYRIGHT © 2011 by the Society of Nuclear Medicine, Inc.

Mononuclear cells were isolated from marrow aspirates by Ficoll-Paque (GE Healthcare) density gradient centrifugation. Cells were counted and cultured in Dulbecco modified Eagle medium/F12 (Gibco Co.) with fetal bovine serum (2%; Hyclone Co.), L-glutamine (2 mmol/L; Hyclone), insulin transferrin selenium (1×; Gibco), dexamethasone ( $10^{-9}$  mol/L; Sigma-Aldrich), ascorbic acid 2-phosphate ( $10^{-4}$  mol/L; Sigma-Aldrich), endothelial growth factor (10 ng/mL), penicillin (100 U/mL), and streptomycin (1,000 U/mL; Gibco) at  $3 \times 10^5$  cells/cm<sup>2</sup> in a humidified incubator at 37°C and 5% CO<sub>2</sub>. The hMSCs adhered to the walls and grew, and nonadherent cells were removed after 24–48 h. Under an inverted-phase microscope, hMSC morphologies included spindle-, triangle-, and polygon-shaped cell types, with clearly visible nuclei and one or more nucleoli.

When the cells reached 80%–90% confluence, they were digested with 0.125% trypsin and replanted in a 1:2 dilution under the same culture conditions. After being subcultured for 6 passages, the cells were digested with trypsin, collected, and prepared for transplantation.

### ICH Modeling

Twenty-four *Macaca fascicularis* monkeys (male, 4–6 y old,  $4.2 \pm 0.2$  kg) were provided by the Experimental Animal Center of the Chinese Academy of Military Medical Sciences. The primate laboratory was licensed and accredited, and all monkeys were acclimated for 2 wk in the animal room before neurologic evaluation. During the experiment, the animals were housed in facilities accredited by the Association for Assessment and Accreditation of Laboratory Animal Care, and the procedures were approved by the institutional animal care and use committee of the Chinese Academy of Medical Sciences (MC-07-6004).

The monkeys were kept fasting overnight, and fluid intake was prohibited for 4 h before surgery. Ketamine (15 mg/kg) and sodium pentobarbital (30 mg/kg) were delivered by intramuscular injection. A heparinized (80 U sodium heparin) blood collection tube was used to collect 2 mL of femoral artery blood from each monkey for autologous injection. The monkey's head was fixed in a Stoelting 51851 stereotactic instrument (Stoelting Co.). The coordinates were recorded, and the coordinate origin was set. Generally, the coordinates were 16 mm in the anteroposterior direction, 16 mm in depth, and 14 mm laterally. The injection point was outside the right putamen, according to a stereotactic map and preoperative MRI of the monkeys. The blood was administered 3 times, 0.5 mL per administration, and the needle stayed in position for 5 min before it was moved 1.5 mm upward for the next administration. When all the blood was injected, the needle remained in position for 15 min more. After surgery, the animals were kept warm using an electric blanket, and their vital signs were monitored until they regained consciousness. Penicillin (400,000 units per day, intramuscularly) was administered for 3 d after surgery. The 24 monkeys were randomly divided into 3 groups, which were designated as the early treatment group ( $n = 8$ ), the late treatment group ( $n = 8$ ), and the control group ( $n = 8$ ). The age and weight of the monkeys was not significantly different among the 3 groups.

### Transplantation Procedure

hMSCs were transplanted using a stereotactic method either 1 wk after ICH modeling (early treatment group,  $n = 8$ ) or 4 wk later (late treatment group,  $n = 8$ ). Animal preparations and anesthesia were the same as described above. Using the same stereo-

tactic instrument and following the original positioning of bone apertures, a microsyringe was used to inject  $(1-5) \times 10^6$  hMSCs in a volume of 250  $\mu$ L to 9 points near the hematoma according to a stereotactic map and MRI. Three tracks of injection were used, and each track had 3 injection points. The first injection point for each track was 3 mm away from the outside edge of the hematoma, and the second and third injection points were chosen by withdrawing to a distance of 1.5 mm from the previous injection point. The injection volume for each point was 25–30  $\mu$ L. The control monkeys were injected with the same volume of saline by the same method, either 1 wk later ( $n = 4$ ) or 4 wk later ( $n = 4$ ). During the procedure, vital signs of the monkeys were monitored. After transplantation, penicillin (400,000 units per day, intramuscularly) was administered for 3 d.

### Behavioral Testing

Scores for neurologic function were refined and modified from the Kito score scale (14,15) and also referenced the “Neurologic Scale for Middle Cerebral Artery Infarction” (16). The scale had a total of 100 scores, including 28 scores for awareness, 22 scores for the sensory system, 32 scores for the movement system, and 18 scores for the coordination of skeletal muscles.

Neurologic functions were evaluated weekly or biweekly (Fig. 1). In each evaluation, the animals were evaluated once in the morning and once in the afternoon, and the behavior of the monkeys was continuously recorded for 24 h with a video recorder. This comprehensive assessment was performed by 2 professionals from the animal center who were not included in the research team and were unaware of the treatment paradigm.

### MRI

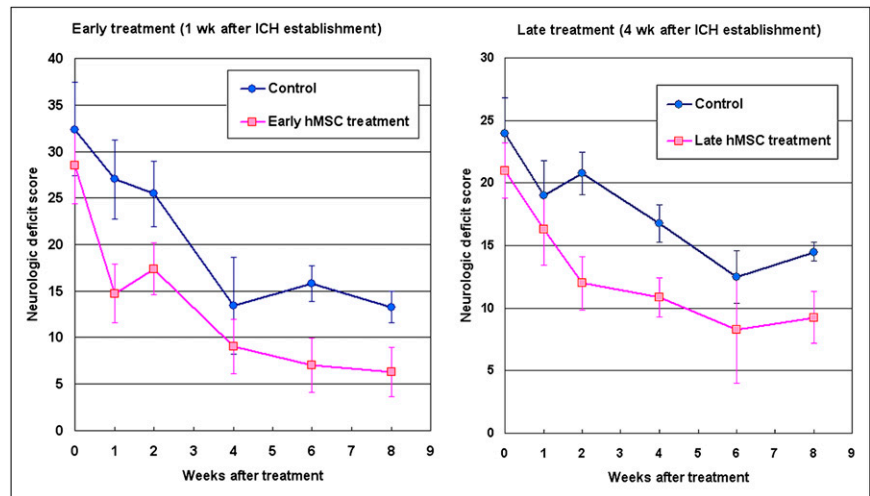
The MRI scan was obtained before the modeling and cell transplantation to assist in the injection positioning. The scans were obtained using an Intera Achiva 3.0-T machine (Philips Healthcare) with 8-channel head coils. Before the scan, the animals were anesthetized using a 15 mg/kg concentration of ketamine and fixed into a magnet-free frame. The T1 scan sequence was inversion recovery; visual field was 120.0 mm; repetition time/echo time (TR/TE) was 2,153/13; slice thickness and interval were 3.0 and 0.3 mm, respectively; matrix was  $256 \times 256$ ; NSA was 6; inversion time was 800 ms; and acquisition time was 16 min 12 s. The sequence of the T2-weighted scan was spin echo; visual field was  $120.0 \times 120.0$  mm; TR/TE was 3,200/102; slice thickness and interval were 3.0 and 0.3 mm, respectively; matrix was  $256 \times 256$ ; NSA was 8; and acquisition time was 17 min 42 s.

### <sup>18</sup>F-FDG PET

The PET scanner was an ECAT EXACT HR+ system (Siemens-CTI), which contained 32 detector rings of bismuth germanate crystal and had a spatial resolution of 5 mm. The PET tracer, <sup>18</sup>F-FDG, was homemade in accordance with good-manufacturing-practice requirements, using an RDS-111 cyclotron and the corresponding radiochemical synthesis system (Siemens-CTI). Quality control was assessed, and the radiochemical purity was higher than 98%.

Because of the difficulty of making arrangements for PET, only 19 monkeys were randomly selected to enroll in the serial PET evaluation from the beginning: 6 were selected from the early treatment group, 6 from the late treatment group, and 7 from the control group (3 were injected with saline 1 wk later and 4 were

**FIGURE 1.** Comparison of neurologic deficit scores (0 = normal, 100 = worst score) between hMSC-treated monkeys and controls. No significant difference was found between hMSC treatment groups and corresponding controls before treatment (week 0). Significantly better scores were observed in both early treatment group ( $P < 0.05$ ) and late treatment group ( $P < 0.01$ ) when data were analyzed with 2-way ANOVA with 1 repeated factor of posttreatment week.



administered saline 4 wk later). The PET was undertaken at 1, 2, 3, 4, 5, 7, and 9 wk after ICH modeling for the early treatment group and at 2, 4, 5, 7, 9, 11, and 13 wk after ICH modeling for the late treatment group (Figs. 2 and 3). There was a time window of  $\pm 3$  d to make arrangements for PET.

The animals (which had been kept fasting for at least 4 h) were anesthetized with ketamine (15 mg/kg), and 37–47 MBq (1.0–1.3 mCi) of  $^{18}\text{F}$ -FDG were injected intravenously. After 28–36 min of distribution, the monkeys underwent a brain-imaging acquisition including 6 min for the 3-dimensional-mode emission scan and 3 min for the transmission scan. The images were reconstructed with optimized parameters and were displayed in a slice thickness of 1.3 mm.

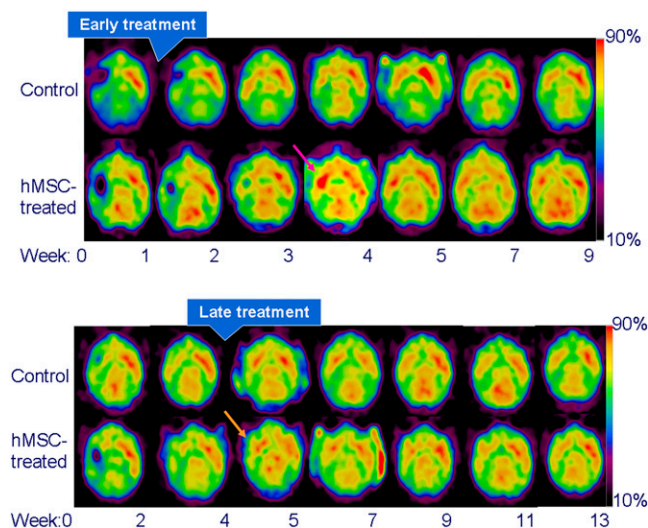


**FIGURE 2.** Serial PET images demonstrating metabolism recovery after ICH establishment. Four typical cases that underwent early (at week 1 after modeling, upper 2 rows) or late (at week 4, lower 2 rows) treatment were shown as control and hMSC-treated monkey brains compared one by one. Pink arrow points to intense  $^{18}\text{F}$ -FDG uptake at hematoma region in early hMSC-treated monkey, and orange arrow shows higher  $^{18}\text{F}$ -FDG accumulation at ipsilateral basal ganglia 1 wk after hMSC injection as early response. Scale was set according to percentage of maximum signal intensity.

The PET images and data were analyzed by 2 independent, experienced staff member who were not aware of the treatment paradigm. They reached a consensus in cases of discrepancy. In the remote workstation of the PET system, the serial PET images obtained from the same monkey were adjusted from the axial, coronal, and sagittal directions and coregistered to reach a standardized and symmetric view and then were resaved as a set of axial images with a standardized slice thickness of 2.6 mm for semiquantitative analysis. A set of ring-shaped regions of interest with a diameter of 3.9 mm was drawn over the slice with the most obvious changes in the first study and then was input into the following images of the registered serial studies, with minor adjustment when the position was changed during recovery (Fig. 3). The mean uptake values (expressed as Bq/mL) of adjacent cortex and basal ganglia were compared with those of mirror regions of the brain. Changes in uptake in the serial PET scans were analyzed by comparing the ratios to the contralateral side (ratio = uptake of a region of interest/uptake of the mirror region of interest) of the matched images (Fig. 3).

### Pathologic Examination

Eight weeks after hMSC transplantation, 2–4 times an anesthetic dose was used to euthanize the monkeys after the neurologic evaluation and PET scans. The animals were lavaged using 500 mL of neutral formaldehyde and 1,500 mL of saline, a craniotomy was performed, and the brain was removed. The brain was divided into 7 pieces and embedded in paraffin for slicing. In the region of the ICH remains, the slice thickness was set to 0.3 cm. The slices were stained with hematoxylin and eosin and observed under a light microscope. An automatic microscope slide scanner (Aperio Technologies) was used to scan the pathologic sections. The microvessel density (MVD) surrounding the remains of the ICH was calculated according to the Weidner method (17). Areas with high vascularization were identified by scanning the hematoxylin- and eosin-stained sections at  $\times 10$  magnification. MVDs were counted in 5 different  $\times 40$  fields, and the mean was considered the final MVD.

### Statistical Analysis

All computations were performed using SPSS 13.0 (SPSS Inc.). The data of neurologic deficit scores and PET were analyzed by 2-way ANOVA with 1 repeated factor of postsurgery time.

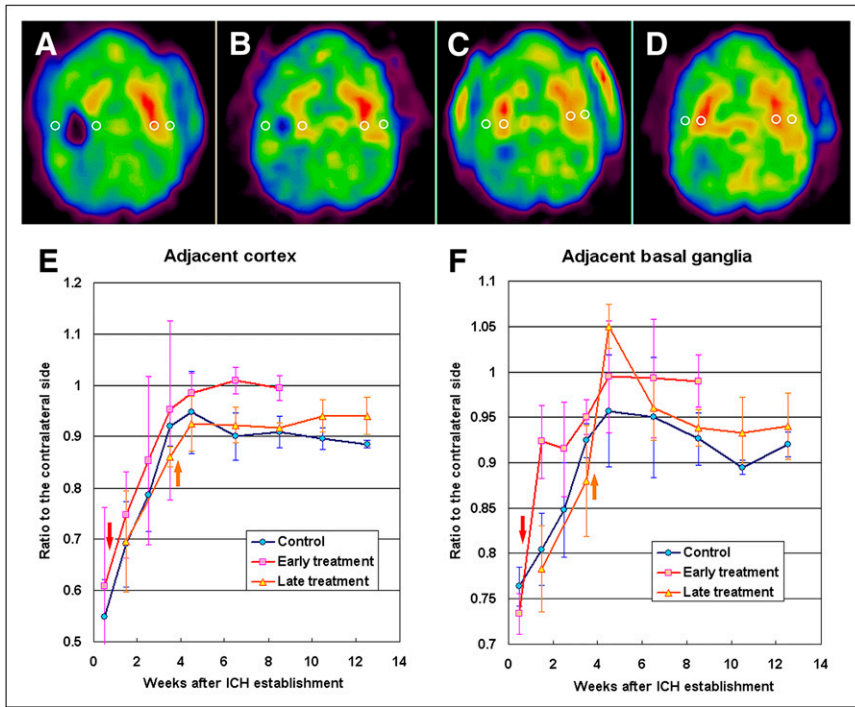


**FIGURE 3.** Demonstration of setting regions of interest over serial PET images (A–D) and metabolic recovery (shown as mean  $\pm$  SD of uptake ratio to contralateral side) according to week after ICH establishment. Adjacent cortex and basal ganglia were evaluated separately (E and F, respectively), and lines connecting means show trend and vertical lines of SD for variability in different groups. Red and orange arrows show time of early and late treatment, respectively.

Pairwise comparison (repeated measures–post hoc multiple comparisons–Bonferroni) was used to test the difference between the pretreatment time point and each posttreatment time point. The data of MVD were analyzed by independent-samples *t* testing. Differences were determined to be significant for *P* values of less than 0.05.

## RESULTS

### Scoring of Neurologic Function

Neurologic functions of the monkeys were evaluated with a modified Kito score scale. Before ICH modeling and hMSC treatment, there was no significant difference in neurologic deficit scoring among the early treatment group, the late treatment group, and the control group. After analysis with 2-way ANOVA with 1 repeated factor, a significant difference was observed between the hMSC treatment groups and the corresponding subgroups of control ( $P < 0.01$  for early treatment and  $P < 0.05$  for late treatment). By pairwise comparison, a significant difference was observed between the pretreatment time point and the 5 posttreatment time points ( $P < 0.05$ ) (Fig. 1).

### $^{18}\text{F}$ -FDG PET Evaluation

Before hMSC transplantation, there was no significant difference in  $^{18}\text{F}$ -FDG uptake among the monkeys of the early treatment group, the late treatment group, and the control group. In the serial follow-up of control monkeys with  $^{18}\text{F}$ -FDG PET, 2 phases of recovery were observed after ICH modeling: a hematoma-absorbing phase that usually lasted 4 wk, followed by a stable phase that indicated a plateau of recovery (Fig. 3). Brain  $^{18}\text{F}$ -FDG uptake did not significantly differ between the control monkeys injected

with saline 1 wk after ICH modeling ( $n = 3$ ) and those injected 4 wk later ( $n = 4$ ) when they underwent  $^{18}\text{F}$ -FDG PET in the same period. Therefore, the 2 subgroups of control monkey were considered as 1 control group ( $n = 7$ ) in statistical analysis.

Compared with the control group, significantly higher  $^{18}\text{F}$ -FDG uptake was observed in the ipsilateral basal ganglia 1 wk after hMSC injection ( $P < 0.05$  for early treatment and  $P < 0.01$  for late treatment) (Fig. 3), and the difference disappeared in both groups during the following weeks. During the transformation from absorbing phase to stable phase, intense  $^{18}\text{F}$ -FDG accumulation surrounding the hematoma appeared in 3 (50%) early hMSC-treated monkeys (Fig. 2). However, the variation in uptake was large within the group, and no significant difference from controls was observed. When the recovery plateaued,  $^{18}\text{F}$ -FDG uptake in the adjacent cortex of the early treatment group became significantly higher than that of the control group ( $P < 0.05$ ) (Fig. 3). The recovery of the ipsilateral basal ganglia was also better in the early treatment group but without significance (Fig. 3). During the stable phase of the late treatment group, the recovery of both adjacent cortex and basal ganglia seemed better than that of the control group. However, there was also no statistical significance between the hMSC-treated and control groups (Fig. 3).

### Pathologic Findings

Pathologic analysis revealed that the hematomas had been almost absorbed in all monkey brains and the remains were linear or spindle-shaped regions with hemosiderin deposition. Under  $\times 40$  magnification, degeneration and necrosis of local cerebral tissue were observed, accompa-

nied by foam cell accumulation, inflammatory cell infiltration, and fibrosis. By visual analysis, the hMSC-treated groups had less tissue damage and more MVD than the control group (Fig. 4). A quantitative analysis of MVD at the remains of the ICH revealed that both the early and the late treatment groups had significantly higher MVD than the control group ( $P = 0.007$  and  $0.014$ , respectively) (Fig. 4).

## DISCUSSION

To the best of our knowledge, this study was the first to use a primate model to evaluate the efficacy of hMSCs in the treatment of ICH and the first to use serial  $^{18}\text{F}$ -FDG PET to evaluate the metabolic recovery of cortex and basal ganglia adjacent to a hematoma after stem cell treatment. The efficacy of hMSC treatment was also demonstrated by 2 other complementary aspects: better recovery of neurologic function as evaluated by a neurologic deficit scoring scale and less damage and higher vessel density surrounding the remains of hematoma as revealed by pathologic analysis. Compared with late hMSC transplantation 4 wk after establishment of an ICH model, early treatment at the first week might lead to a better result.

The pathologic processes after an ICH are complicated. An ICH can induce neurologic damage by local tissue deformation and subsequent development of excitotoxicity, apoptosis, and inflammation (18). Transplantation of mesenchymal stem cells (MSCs) might promote neuroprotection and functional recovery by several mechanisms as demonstrated by previous studies. First and to a large extent, the therapeutic potential of MSCs may rely on their

differentiation ability. However, new findings suggest that the ability of MSCs to alter the tissue microenvironment occurs via secretion of soluble factors that may contribute more to tissue repair (19). MSCs can also regulate angiogenesis by a process dependent on fibroblast growth factor receptor and vascular endothelial growth factor receptor signaling cascades, as well as additional cross-talk with other pathways (20). In addition, transplanted allogenic MSCs can induce immune tolerance, which may be therapeutic for the alleviation of graft-versus-host disease, transplantation rejection, and the modulation of inflammation (21). Therefore, MSCs hold great promise for the treatment of ICH.

However, translational research about treatment of an ICH with MSCs has been limited. The few previous investigations, mostly with the rat ICH model, indicated that MSCs might differentiate into neural cells (9), stimulate endogenous progenitor cells (10), and induce antiinflammatory and angiogenesis effects (11,12). Also, MSCs reduced chronic brain degeneration and promoted long-term functional recovery. The benefits were even observed in rat models treated with human-derived MSCs (10–12). To move the translational process forward, this study used a primate ICH model of *Macaca fascicularis* monkey; the hMSCs were injected using a stereotactic method near the hematoma; the efficacy of treatment was evaluated by observing the recovery of glucose metabolism of the surrounding cortex and basal ganglia through serial  $^{18}\text{F}$ -FDG PET; and 2 other complimentary approaches were also combined, including a neurologic deficit scoring to monitor

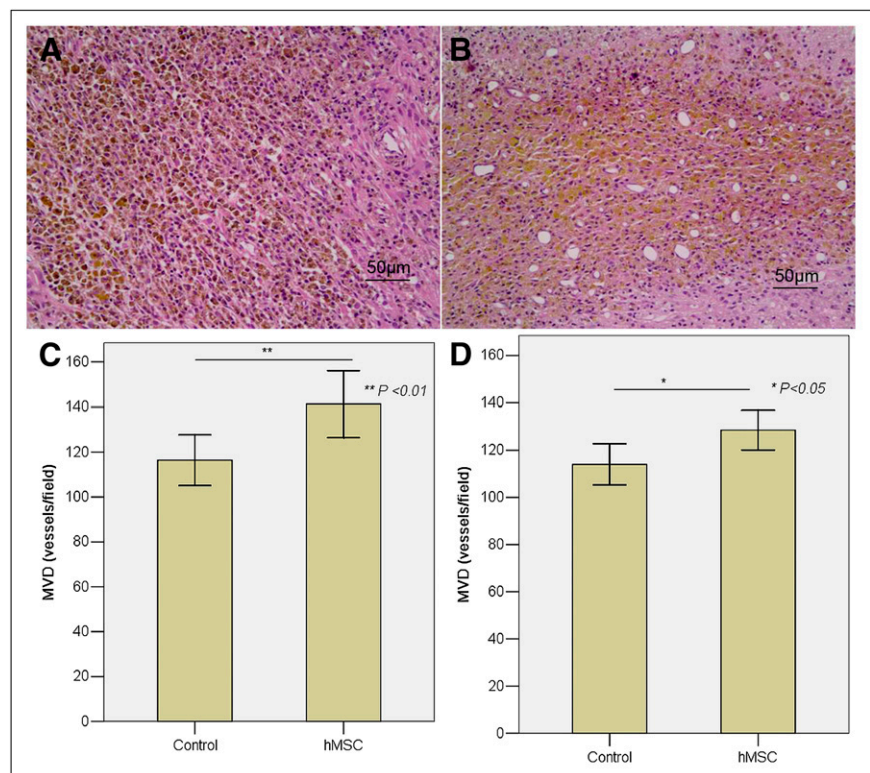


**FIGURE 4.** Hematoxylin and eosin staining ( $\times 40$ ) of ICH remnants (A: control; B: hMSC-treated) and comparison of MVD at ICH remnants between early treatment group and corresponding control (C) and between late treatment group and its control (D).

the functional recovery of the monkey and a pathologic analysis to reveal changes in the brains at the end of the study.

Serial  $^{18}\text{F}$ -FDG PET was used to evaluate cerebral glucose metabolism after ICH modeling. A transient early response was observed 1 wk after transplantation in both the early and the late treatment groups, which was characterized by significantly higher  $^{18}\text{F}$ -FDG accumulation in the ipsilateral basal ganglia. At 6 and 8 wk after hMSC transplantation, when recovery plateaued, significantly better recovery was found at the adjacent cortex in the early treatment group. Recovery also appeared to have improved at the adjacent basal ganglia in the early treatment group and at both adjacent cortex and basal ganglia in the late treatment group, but these findings were not statistically significant, possibly because of the small number of animals. In addition, remarkably higher levels of  $^{18}\text{F}$ -FDG accumulated around the hematoma during the peak of repair in some early hMSC-treated monkeys. No similar phenomenon was observed in the controls and the late treatment group. These data indicated that the hMSCs transplanted into the brain by the stereotactic method might have improved the recovery of the monkeys from an experimental ICH, especially in the early treatment group.

The neurologic function scores were also significantly better in both early and late treatment groups. We adopted a modified neurologic deficit score scale (Table 1) that was more detailed and easier to operate than the Kito score scale (14). The scale included an evaluation of consciousness, skeletal muscle coordination, sensory system function, and motor system function. To be more objective, the assessment was conducted by 2 researchers who were unaware of the treatment paradigm. However, we still found that the scores varied widely within each group. The largest variation was at the fourth week after hMSC transplantation in the early treatment group, which also varied widely when evaluated with  $^{18}\text{F}$ -FDG PET. In addition, better results were also found in the early treatment group than in the late treatment group, especially at the later period of the stable phase.

Pathologic analysis revealed less degeneration in the brain specimens of the hMSC-treated monkeys but significantly higher MVD near the remains of an ICH. A previous study using  $\text{Flk1}^+$  hMSCs suggested the cells could potentially develop into hematoangioblasts and generate endothelial cells to promote neovascularization (22). A recent study using human umbilical cord-derived MSCs to treat ICH in a rat model also revealed significantly higher vascular density in the peri-ICH area, and transplanted MSCs were observed becoming incorporated into the cerebral vasculature (11). Thus, the neovascularization might have increased the local blood supply and exerted a neuroprotective function. In addition, we observed intense  $^{18}\text{F}$ -FDG accumulation around the hematoma at the end of the absorbing phase in 3 early hMSC-treated monkeys. It is an interesting phenomenon, and further investigation is

needed to define whether it is due to the angiogenesis, neuroprotection, and even neuroactivation mechanisms of MSC or is simply an inflammatory process.

The current study has some limitations: First, because the hMSCs are not labeled, their survival and migration cannot be tracked either by imaging during the recovery or by histologic analysis at the end of observation. Therefore, it is difficult to determine the mechanism of the observed differences among the groups. However, an early response to hMSC treatment was observed in this study, indicating that a microenvironment change might contribute to tissue protection and repair; and the pathology at the end of the study proved the treatment-related angiogenesis, which might play a role during the recovery. Second, the ICH model, produced by the stereo-guided injection of autologous arterial blood into the space outside the right putamen, might be different from that caused by cerebral artery disease. Some researchers prefer to establish an ICH model with bacterial collagenase, which could disrupt the basal lamina of cerebral blood vessels and cause blood leakage into the surrounding tissue (9–12). However, other researchers argue that collagenase can produce an exaggerated inflammatory response and is directly toxic to neurons (23). Moreover, the induced hemorrhage is clearly not easy to control. On the other hand, injection of autologous blood into the brain parenchyma can preferentially simulate the pathologic changes observed during ICH (24,25), and the volume of hematoma can be standardized by stereotactic injection of a suitable volume of autologous blood to a specific region of brain. In the preexperiment, we found that 1.5 mL was a suitable volume to produce an obvious neurologic deficit without killing any of the monkeys. This volume of blood in the brain of a *Macaca fascicularis* monkey was equivalent to a 30-mL hematoma in an adult human brain, which was near the highest amount for a conservative treatment of hematoma (3). To prevent reflux from the path of the injection needle, some researchers have used the method of 2 blood injections (24,25). In this study, a 3-injection method was adopted, and the needle stayed in position for 5 min after each injection; after all 3 blood injections, the needle remained in position for 15 min more to warrant no reflux. The third limitation was that the monkeys were observed only 8 wk after hMSC transplantation. Although a relatively stable phase of recovery had been reached 6 wk after transplantation, the observation period was still not enough. The long-term effects of hMSC treatment await further investigation.

## CONCLUSION

This study indicated the benefit of early stereotactic transplantation of hMSCs in a primate model of ICH by serial  $^{18}\text{F}$ -FDG PET, neurologic function scoring, and pathologic analysis. The efficacy reported in this article and the safety of hMSC transplantation may warrant further translational research on promoting the hMSC treatment for ICH in humans.

**TABLE 1**  
Neurologic Deficit Score for Monkeys After Stroke

Category	Score
<b>Consciousness</b>	
Normal, consistently alert, strongly aggressive, escape-prone	0
Conscious but clouded, strongly aggressive	2
Conscious, poorly aggressive	4
Conscious, light opposition, escape-prone	6
Conscious but clouded and accepting	8
Drowsiness, aroused with stimulation	10
Lethargic, eyes open by strong stimulation	16
Stuporous, aroused with persistent stimulation	20
Light coma, reflex movement only	24
Deep coma, no movement	28
<b>Skeletal muscle coordination</b>	
Normal, walks normally	0
Light, transient abnormality in motor coordination	2
Minimal ataxia, walks with some impairment of gait	4
Ataxia but able to climb the cage	6
Walks with compelling stimulation but has difficulty in climbing the cage	8
Stands spontaneously, falls within a few steps	10
Sits, just able to circle with compelling stimulation	12
Sits or prostrate, cannot stand or sit for long duration, with response to compelling stimulation	14
Posed lateral or dorsal recumbency, with response to compelling stimulation	16
No movement, almost with no response to compelling stimulation	18
<b>Sensory system</b>	
Facial sensation (ipsi-/contralateral, 0–3 × 2)	
Concerted reaction to compelling stimulation (aggression, threaten, escape-prone, expressing goodwill)	0/0
Decrease in concerted reaction to compelling stimulation (obvious decreases in aggressive or threatening expressions)	1/1
Decrease in concerted reaction to compelling stimulation (obvious decreases in expressing goodwill)	2/2
Absent, does not react to compelling stimulation in any area of face	3/3
Pinna reflex (ipsi-/contralateral, 0–3 × 2)	
Twitches ear normally	0/0
Slight reduction in ear twitching, twitches ear by sonic stimulation	1/1
Obvious reduction in ear twitching, no ear twitching by sonic stimulation	2/2
Absent, does not move ear by contact stimulation	3/3
Pain reflex (lower limb, ipsi-/contralateral, 0–5 × 2)	
Strong, quick, complete withdrawal by contact stimulation	0/0
Comparatively quick withdrawal by contact stimulation	1/1
Comparatively slow withdrawal by contact stimulation	2/2
Weak, slow, incomplete, or inconsistent withdrawal by contact stimulation	3/3
Very weak, slow withdrawal by contact stimulation	4/4
Absent, no withdrawal by contact stimulation	5/5
<b>Motor system</b>	
Hand (ipsi-/contralateral, 0–4 × 2)	
Normal	0/0
Light dyskinesia (slow velocity, poor strength, and parasequity)	1/1
Reduced strength or skill (comparatively obvious dyskinesia)	2/2
Obvious dyskinesia (very slow velocity, very poor strength, and parasequity)	3/3
Paralysis or useless	4/4
Leg (ipsi-/contralateral, 0–6 × 2)	
Normal	0/0
Light dyskinesia (slow velocity, poor strength, and parasequity)	1/1
Raises with flexion of knee (comparatively obvious dyskinesia)	2/2
Obvious dyskinesia (very slow velocity, very poor strength, and parasequity)	3/3
Can move, but not against gravity	4/4
Almost cannot move	5/5
Paralysis or useless	6/6
Upper-limb tone (ipsi-/contralateral, 0–3 × 2)	
Normal	0/0
Lightly spastic or flaccid (occasionally raised fingers when grasping)	1/1
Relatively spastic or flaccid (continued to raise fingers when grasping)	2/2
Obviously spastic or flaccid	3/3
Lower-limb tone (ipsi-/contralateral, 0–3 × 2)	
Normal	0/0
Lightly spastic or flaccid (occasionally raised toes when grasping)	1/1
Relatively spastic or flaccid (continued to raise toes when grasping)	2/2
Obviously spastic or flaccid	3/3

## ACKNOWLEDGMENT

This work was supported by a grant from the National High-Tech Research and Development Project funded by the Ministry of Science and Technology, P.R. China (2006AA02A115).

## REFERENCES

1. Broderick J, Connolly S, Feldmann E, et al. Guidelines for the management of spontaneous intracerebral hemorrhage in adults: 2007 update: a guideline from the American Heart Association/American Stroke Association Stroke Council, High Blood Pressure Research Council, and the Quality of Care and Outcomes in Research Interdisciplinary Working Group. *Stroke*. 2007;38:2001–2023.
2. Heiskanen O. Treatment of spontaneous intracerebral and intracerebellar hemorrhages. *Stroke*. 1993;24:194–195.
3. Qureshi AI, Tuhim S, Broderick JP, Batjer HH, Hondo H, Hanley DF. Spontaneous intracerebral hemorrhage. *N Engl J Med*. 2001;344:1450–1460.
4. Lyden PD, Zivin JA. Hemorrhagic transformation after cerebral ischemia: mechanisms and incidence. *Cerebrovasc Brain Metab Rev*. 1993;5:1–16.
5. The NINDS t-PA Stroke Study Group. Intracerebral hemorrhage after intravenous t-PA therapy for ischemic stroke. *Stroke*. 1997;28:2109–2118.
6. Jeong SW, Chu K, Jung KH, Kim SU, Kim M, Roh JK. Human neural stem cell transplantation promotes functional recovery in rats with experimental intracerebral hemorrhage. *Stroke*. 2003;34:2258–2263.
7. Lee HJ, Kim KS, Kim EJ, et al. Brain transplantation of immortalized human neural stem cells promotes functional recovery in mouse intracerebral hemorrhage stroke model. *Stem Cells*. 2007;25:1204–1212.
8. Lee ST, Chu K, Jung KH, et al. Anti-inflammatory mechanism of intravascular neural stem cell transplantation in haemorrhagic stroke. *Brain*. 2008;131:616–629.
9. Zhang H, Huang Z, Xu Y, Zhang S. Differentiation and neurological benefit of the mesenchymal stem cells transplanted into the rat brain following intracerebral hemorrhage. *Neurol Res*. 2006;28:104–112.
10. Fatar M, Stroick M, Griebel M, et al. Lipoaspirate-derived adult mesenchymal stem cells improve functional outcome during intracerebral hemorrhage by proliferation of endogenous progenitor cells stem cells in intracerebral hemorrhages. *Neurosci Lett*. 2008;443:174–178.
11. Liao W, Zhong J, Yu J, et al. Therapeutic benefit of human umbilical cord derived mesenchymal stromal cells in intracerebral hemorrhage rat: implications of anti-inflammation and angiogenesis. *Cell Physiol Biochem*. 2009;24:307–316.
12. Kim JM, Lee ST, Chu K, et al. Systemic transplantation of human adipose stem cells attenuated cerebral inflammation and degeneration in a hemorrhagic stroke model. *Brain Res*. 2007;1183:43–50.
13. Fang B, Liao L, Shi M, Yang S, Zhao RC. Multipotency of Flk1<sup>+</sup> CD34<sup>-</sup> progenitors derived from human fetal bone marrow. *J Lab Clin Med*. 2004;143:230–240.
14. Kito G, Nishimura A, Susumu T, et al. Experimental thromboembolic stroke in cynomolgus monkey. *J Neurosci Methods*. 2001;105:45–53.
15. Natale JE, Schott RJ, Hall ED, Braughler JM, D'Alecy LG. Effect of the amino-steroid U74006F after cardiopulmonary arrest in dogs. *Stroke*. 1988;19:1371–1378.
16. Edwards DF, Chen YW, Diringer MN. Unified Neurological Stroke Scale is valid in ischemic and hemorrhagic stroke. *Stroke*. 1995;26:1852–1858.
17. Weidner N. Intratumor microvessel density as a prognostic factor in cancer. *Am J Pathol*. 1995;147:9–19.
18. Aronowski J, Hall CE. New horizons for primary intracerebral hemorrhage treatment: experience from preclinical studies. *Neurol Res*. 2005;27:268–279.
19. Phinney DG, Prockop DJ. Concise review: mesenchymal stem/multipotent stromal cells: the state of transdifferentiation and modes of tissue repair—current views. *Stem Cells*. 2007;25:2896–2902.
20. Kasper G, Dankert N, Fischer J, et al. Mesenchymal stem cells regulate angiogenesis according to their mechanical environment. *Stem Cells*. 2007;25:903–910.
21. Aggarwal S, Pittenger MF. Human mesenchymal stem cells modulate allogeneic immune cell responses. *Blood*. 2005;105:1815–1822.
22. Guo H, Fang B, Liao L, et al. Hemangioblastic characteristics of fetal bone marrow-derived Flk1(+)CD31(-)CD34(-) cells. *Exp Hematol*. 2003;31:650–658.
23. MacLellan CL, Silasi G, Poon CC, et al. Intracerebral hemorrhage models in rat: comparing collagenase to blood infusion. *J Cereb Blood Flow Metab*. 2008;28:516–525.
24. Nan Z, Grande A, Sanberg CD, Sanberg PR, Low WC. Infusion of human umbilical cord blood ameliorates neurologic deficits in rats with hemorrhagic brain injury. *Ann N Y Acad Sci*. 2005;1049:84–96.
25. Xi G, Keep RF, Hoff JT. Erythrocytes and delayed brain edema formation following intracerebral hemorrhage in rats. *J Neurosurg*. 1998;89:991–996.